

## Solid-phase epitaxy of amorphous silicon induced by electron irradiation at room temperature

G. Lulli and P. G. Merli

*Istituto di Chimica e Tecnologia dei Materiali e Componenti per l'Elettronica (LAMEL), Consiglio Nazionale delle Ricerche, Via de'Castagnoli 1, I-40126 Bologna, Italy*

M. Vittori Antisari

*Divisione Scienza dei Materiali, Comitato Nazionale per la Ricerca e per lo sviluppo dell'Energia Nucleare e delle Energie Alternative (ENEA), Centro Ricerche Energetiche della Casaccia, Casella Postale 2400, I-00100 Roma, Italy*

(Received 7 April 1987)

The technique of cross-sectional electron microscopy has been used to investigate the mechanism of electron-beam-induced solid-phase epitaxy of amorphous silicon at room temperature. Cross sections of samples with surface and buried amorphous layers were irradiated in a transmission electron microscope with electrons of energies higher than the threshold energy for atomic displacement and the induced recrystallization process was characterized. Evidence is given that the dominant mechanism of recrystallization is the diffusion to the amorphous-crystalline interface of the defects produced by elastic displacements both in the crystalline and in the amorphous region. The diffusion length of such defects results in the order of 25–30 nm and is approximately the same in the crystalline and amorphous Si. Electron-beam irradiation is shown to induce room-temperature polycrystalline nucleation in the amorphous layer. Such a process becomes competitive with solid-phase epitaxy for a dose higher than  $5 \times 10^5$  C/cm<sup>2</sup>.

### I. INTRODUCTION

The rapid developments of very-large-scale integration (VLSI) technology call for a better understanding and control of the processes used for manufacturing electronic devices. The new interest in the details of beam-target interaction during ion implantation of semiconductors is mainly due to the following reasons: (i) the introduction of new, high-energy, high-current implantation machines; (ii) the problems raised by focused implantation in maskless ion microlithography; (iii) the use of implantation for producing buried insulating layers in silicon-on-insulator (SOI) technology; (iv) the observation of enhanced solid-phase epitaxial growth of amorphous silicon during ion bombardment. The detailed investigations which have been recently carried out about this last item are also related to its possible application in the field of low-temperature processes.

The effect of low-temperature, particle-induced recrystallization of Si and Ge has been known for several years.<sup>1</sup> More recently, in order to clarify the basic mechanism of ion-induced recrystallization, both irradiation of preamorphized Si samples, performed at uniform temperature (ion-beam annealing),<sup>2,3</sup> and high current density implants on virgin samples, for which doping and annealing occur during the same implantation cycle (self-annealing),<sup>4–6</sup> have been performed. In the latter case the temperature rise is due to the heating effect of the ion beam itself. In both kinds of experiments recrystallization is found to occur at temperatures much lower than the value necessary to observe some appreciable thermal epitaxy in a furnace (i.e., about 500°C). The mechanism of such phenomenon has been mainly ascribed to the migration and recombination at the amorphous-crystalline interface of defects created by the

elastic collisions between beam ions and target atoms.<sup>2</sup>

In spite of the efforts which have been devoted to understand the basic mechanism of particle-induced recrystallization, some controversial points still remain to be clarified. The main one “deals with which part of the material the recrystallization occurs in: in the amorphous phase; at the interface; in the crystalline part near the interface; or in two, or in all of these parts.”<sup>7</sup> For instance Williams *et al.*<sup>8</sup> conclude from their experiment that “displaced atoms lead to multiple rearrangements of surrounding atoms, and that the measured activation energy of 0.24 eV is associated with subsequent crystallization processes around these nucleation sites generated at the interface by nuclear collisions of the ion beam.” Linnros *et al.*<sup>7</sup> perform a similar experiment (irradiation of a buried amorphous layer under channeling and random conditions), but give the different conclusion that “the regrowth mechanism involves generation and migration of point defects predominantly in the crystalline part of the material.”<sup>7</sup> The measured activation energy of the process which is about 0.3 eV leads them to identify these defects as neutral vacancies.

A consequence of the hypothesis of a displacement-induced recrystallization is that a similar effect should be observed for irradiation with electrons of energy  $E > E_d$ , where  $E_d$  is the threshold energy for atomic displacement in silicon [i.e., about 145 keV (Ref. 9)]. The results of some experiments reported in the literature seem to confirm the above hypothesis.<sup>10–14</sup> Recently, epitaxial regrowth of implanted Si layers in the temperature range  $400 < T < 500$  °C has been observed for irradiation with 0.8-MeV electrons,<sup>13</sup> while a room-temperature recrystallization obtained by 2-MeV irradiation of a cross-sectional sample in a high-voltage electron microscope (HVEM) has been reported by the authors.<sup>14</sup>

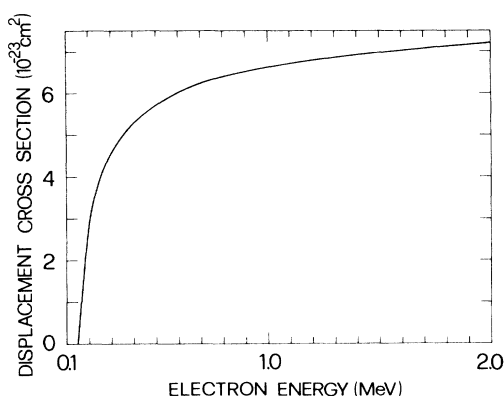


FIG. 1. Cross section for elastic displacement in Si, as a function of electron energy, calculated according to McKinley and Feshbach (Ref. 15).

The aim of the present work is to give a further insight into the mechanism of particle-induced recrystallization, by room-temperature electron irradiation of cross-sectional specimens performed in a transmission electron microscope (TEM) working at 200 and 100 kV. The comparison with the results obtained at 2 MeV allows us to check the role of elastic displacements. In fact the number of primary displacements per atom is given by  $N_d = \phi \sigma_d$ , where  $\phi$  is the dose and  $\sigma_d$  is the displacement cross section which, according to the approximation of McKinley and Feshbach<sup>15</sup> varies with energy as reported in Fig. 1.

Moreover, the results obtained by irradiating the cross section of a sample which exhibits a buried amorphous layer, give crucial information about the origin of the defects which take part in the recrystallization process.

## II. EXPERIMENTAL PROCEDURE

The cross-sectional specimens were prepared from samples obtained in self-annealing experiments which have been described elsewhere.<sup>5,6</sup> To summarize, the implantation was carried out on (100), *p*-type, thermally insulated Si samples, with 100-keV  $P^+$  ions at current densities of 60 to 240  $\mu\text{A}/\text{cm}^2$ . Irradiation times were 5 and 1 s, respectively, giving a total dose of  $1.9 \times 10^{15}$  and  $1.5 \times 10^{15}$  atoms/ $\text{cm}^2$ . In the former case the combined effect of amorphization and self-annealing produces a buried amorphous layer 100 nm thick with a surface crystalline layer 40 nm thick. The result of implantation in the latter conditions was a continuous amorphous layer 200 nm thick.

Electron irradiations were performed with a JEOL 200B electron microscope, equipped with a  $\text{LaB}_6$  cathode and operating up to 200 kV. Beam current density was measured by a Faraday cage, installed in the observation chamber of the microscope; the collected current was amplified by a Keithley 427 current amplifier. The measurements were performed on the central part of the spot, over an area with a diameter of  $\sim 150$  nm. In this region, which is small compared to the spot diameter ( $\sim 2 \mu\text{m}$ ) the beam current density is practically homogeneous. The microscope was operated

with the first condenser lens off and with only the fixed condenser aperture intercepting the electron beam. This experimental setup allows current densities at the specimen plane as high as 150  $\text{A}/\text{cm}^2$ . The irradiation time required for a complete recrystallization was generally less than 1.5 h. Pictures of the irradiated area were taken every 5 or 10 min. At the same time the current density was monitored and recorded.

In order to estimate the effect of beam heating of the specimen the following expression was used:<sup>16</sup>

$$T_{\max} - T_0 = \frac{J}{2ek} \frac{dE}{dx} \left[ \ln \frac{R}{r_0} + \frac{1}{2} \right] r_0^2, \quad (1)$$

where  $(T_{\max} - T_0)$  is the maximum temperature rise induced by a uniform spot of radius  $r_0$  and current density  $J$ , impinging on a circular sample of radius  $R$ , which is kept in good thermal contact at its periphery with a holder at  $T = T_0$ .  $k$  is the thermal conductivity of the specimen,  $e$  is the electron charge,  $dE/dx$  is the electronic stopping power of the specimen. If we take  $dE/dx = 7.5 \times 10^{-13} \text{ J cm}^{-1}$  for 200 keV electrons,<sup>16</sup> and consider the typical range of parameters used in our experiments ( $r_0 \approx 1 \mu\text{m}$ ,  $J \leq 110 \text{ A}/\text{cm}^2$ ,  $R \approx 1 \text{ mm}$ ) we calculate that, for  $k = 1.5 \text{ W cm}^{-1} \text{ K}^{-1}$ , which is the value of thermal conductivity of crystalline Si, beam heating effects are negligible. This conclusion was experimentally confirmed by irradiating a sample with a beam energy of 100 keV, which is lower than the displacement threshold for Si, and a current density of 110  $\text{A}/\text{cm}^2$ . No detectable recrystallization was observed, even after an irradiation time of several hours. Moreover, as will be seen later, the comparison of recrystallization rate observed for different current densities at 200 keV, shows that the width of the regrown layer depends only on the total electron dose and not on the dose rate. These observations leave out the possibility that some epitaxial growth of thermal nature can take place during the irradiation of the specimens.

## III. RESULTS AND DISCUSSION

Figure 2 shows the thickness of the regrown layer versus electron dose for the irradiation of the cross-sectional sample with a surface amorphous layer 200 nm thick. The irradiation was performed at a current density of  $\sim 105 \text{ A}/\text{cm}^2$ . For comparison the data from 2 MeV electron irradiations at 4  $\text{A}/\text{cm}^2$  are reported in the same figure.

The behavior of regrown layer thickness versus dose is linear up to a distance of about 120 nm from the surface. In this region the ratio of the recrystallization speeds for irradiation at 2 and 0.2 MeV is practically equivalent to the ratio of the primary displacement cross sections (see Fig. 1).<sup>17</sup> This fact, together with the absence of regrowth observed for 100 keV irradiation, gives further evidence of the elastic displacement as the dominating

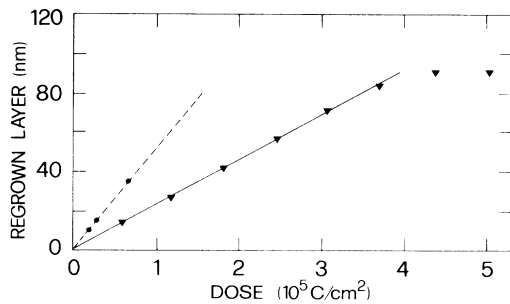


FIG. 2. Regrown layer thickness vs electron dose for irradiations with 200 keV electrons at current density of 105 A/cm<sup>2</sup> (▼) and for irradiation with 2 MeV electrons at a current density of 4 A/cm<sup>2</sup> (●).

mechanism of particle induced recrystallization.

At a distance of about 110 nm from the surface, when the dose reaches the value of  $\sim 5 \times 10^5$  C/cm<sup>2</sup>, the recrystallization process is stopped abruptly. Figure 3 shows a cross section of the sample under consideration in an unirradiated region and in the irradiated region, after the interface has stopped. The diffraction pattern reported in the inset, shows that polycrystalline nucleation has occurred in the surface amorphous layer 100 nm thick, before complete epitaxial growth could take place. This polynucleation is the cause of the interface stopping.

The competition between solid phase epitaxy and polycrystalline nucleation in ion-implanted Si during thermal annealing has been extensively investigated.<sup>20,21</sup> It has been observed that, for low-dopant concentration ( $C < 10^{20}$  atoms/cm<sup>3</sup>) and temperatures not exceeding 1350 °C, solid-phase epitaxy is the dominant process due to its lower thermal activation energy ( $E_a \approx 2.5$  eV, compared to  $E_a \approx 4$  eV for polynucleation). The presence of impurity precipitates in the amorphous layer, in the case of high-dose implantation, may favor polynucleation. When such nucleation occurs the amorphous-crystalline interface may be slowed down and ultimately stopped as it approaches the region where polycrystalline material has been formed. For the experimental conditions (im-

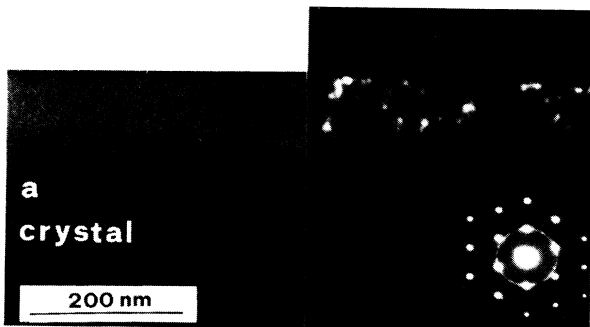


FIG. 3. TEM micrographs of a cross section of the sample irradiated at 200 keV under conditions described in Fig. 2. Left side, unirradiated area (bright-field image); a, amorphous region; right side, picture of the area irradiated with a dose of  $5 \times 10^5$  C/cm<sup>2</sup>. The latter picture is a dark-field image obtained using a portion of a polycrystalline ring present in the diffraction pattern reported in the inset.

planted dose and irradiation temperature) relative to the sample shown in Fig. 3, the previous mechanism seems unlikely.

It is well known that irradiation with high-energy particles may induce phase transformations in materials. The possibility, for instance, that irradiation can enhance the atomic rearrangement leading to crystallization of an amorphous material has been considered.<sup>22</sup> In the present case it is interesting to point out how the two different processes (solid phase epitaxy and polynucleation) are affected by electron irradiation. If we make a comparison with the observed behavior during thermal processing at high temperature, we can say that under electron-beam irradiation at room temperature, the kinetics of polynucleation is apparently more strongly enhanced than the kinetics of solid-phase epitaxy.

Figure 4 illustrates the behavior of regrown layer as a function of electron dose for irradiation of the sample which exhibits a buried amorphous layer 100 nm thick. To check the influence of dose rate, irradiations were performed at current densities of 76, 93, and 108 A/cm<sup>2</sup>. The behavior of upper as well as of deep interface is displayed. For comparison the data referring to the regrowth of a single amorphous-crystalline (*a-c*) interface are reported too. The main points to be underlined are (i) no appreciable influence of dose rate is observed; (ii) after a difference observed at the early stage of the process, the regrowth rates for upper and deep *a-c* interfaces are the same; (iii) the regrowth rate of the deep *a-c* interface is initially equal to the regrowth rate observed in the sample with a single interface, but is progressively slowed down, as the recrystallization proceeds.

To clarify this last point we have reported in Fig. 5 the regrowth rate expressed as the regrown layer thickness for a unit dose of 1 C/cm<sup>2</sup>, as a function of the buried amorphous layer thickness. The point relative to the sample with a single *a-c* interface is reported too. We will discuss later the lower regrowth rate observed at the early stage of the process for the upper *a-c* interface. First of all we consider the range where the velocities of the two growing interfaces are the same. The most in-

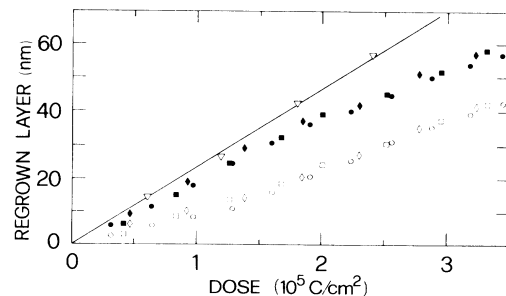


FIG. 4. Regrown layer thickness vs electron dose for irradiation of the sample with a buried amorphous layer, performed at 200 keV and different current densities  $J$ . Open symbols refer to upper amorphous crystalline interface, while solid ones refer to the deep interface.  $\diamond, \square, \circ, \bullet$ :  $J = 76$  A/cm<sup>2</sup>;  $\square, \bullet$ :  $J = 93$  A/cm<sup>2</sup>;  $\circ, \bullet$ :  $J = 108$  A/cm<sup>2</sup>. Open triangles ( $\nabla$ ) refer to the regrown behavior of the sample with a single amorphous crystalline interface (see Fig. 2).

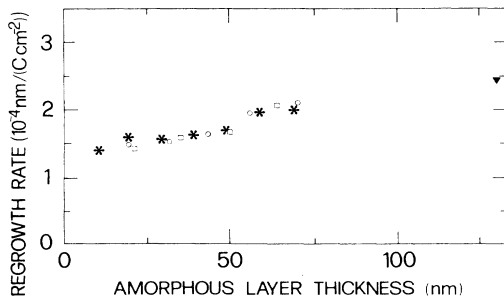


FIG. 5. Solid-phase epitaxial rate as a function of the amorphous-layer thickness for the sample with a buried amorphous layer irradiated at three different current densities  $J$ ;  $\square$ :  $J = 76 \text{ A/cm}^2$ ;  $\circ$ :  $J = 93 \text{ A/cm}^2$ ;  $*$ :  $J = 108 \text{ A/cm}^2$ . The data refer to the movement of the deeper interface. For comparison the point relative to the regrowth rate observed for the sample with a single amorphous-crystalline interface is reported too ( $\blacktriangledown$ ).

interesting feature of the results shown in Figs. 4 and 5 is the slowing down of the interface velocities as the thickness of the amorphous layer is reduced. For a thickness of  $\sim 50 \text{ nm}$  the difference with the rate observed for the single  $a$ - $c$  interface growth becomes manifest. The growth rate reduces progressively to about one half of its initial value, as shown in Fig. 5.

It should be pointed out that a similar effect had already been observed in self-annealing experiments, when a buried layer with two growing interfaces were present.<sup>5</sup> If we assume that the regrowth rate is proportional to the number of defects which are available at the interface, we must hypothesize a reduction of defects supply with decreasing the amorphous layer thickness.

The most satisfactory and simple hypothesis which can, in our opinion, explain such experimental behavior is that defects coming with a diffusive process both from the amorphous and from the crystalline region, contribute to the recrystallization at the interface. Under such an assumption we expect that the regrowth rate will begin to decrease when the amorphous layer thickness will become of the order of  $2\lambda_a$ , where  $\lambda_a$  indicates the diffusion length in the amorphous Si of the defects which are responsible for recrystallization. From the data reported it is possible to infer a diffusion length of the order of 25–30 nm. Moreover, the observation that the velocity of the interfaces extrapolated to zero amorphous-layer thickness is about one-half of the velocity of the single interface (Fig. 5), leads us to conclude that the contributions to regrowth coming from the crystalline and from the amorphous regions must be approximately the same.

The lower regrowth rate detected for the upper interface at the early stage of recrystallization (Fig. 4) may be explained as well. In fact the reduced defects supply can be attributed to the thickness of the surface crystalline layer, which is initially lower than  $2\lambda_c$ , where  $\lambda_c$  indicates the diffusion length of defects in the crystal. This leads to a reduced contribution from the crystalline side. As the two interfaces show the same regrowth rate when the surface crystalline layer thickness becomes greater than  $\sim 50 \text{ nm}$  we can conclude that  $\lambda_c \simeq 25 \text{ nm} \simeq \lambda_a$ .

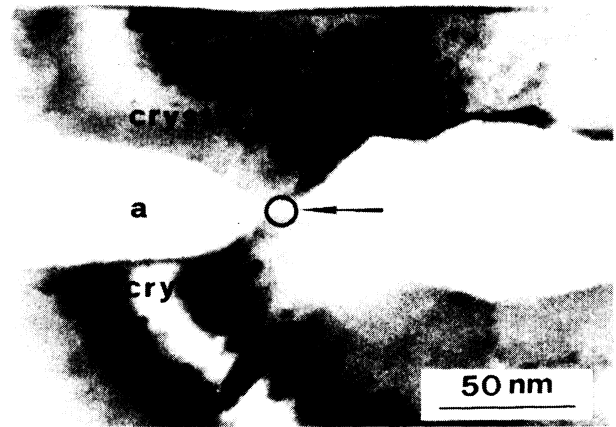


FIG. 6. TEM bright-field image of the sample irradiated at the center of the buried amorphous layer for a time of 15 min with a beam diameter of 10 nm. The arrow shows the beam impact region while the small ring represents the beam size; a, amorphous region. Beam energy was 200 keV. The current density was estimated of the order of  $300 \text{ A/cm}^2$ .

To give further evidence of a regrowth mechanism based on point defects diffusion, we present a preliminary result of an experiment which will be discussed in detail elsewhere.<sup>23</sup> We have irradiated a sample exhibiting a buried amorphous layer about 60 nm thick in a 200 kV scanning transmission electron microscope. Beam spot was reduced to a diameter of 10 nm, and localized entirely inside the amorphous region, at the center of the buried layer, while current density was of the order of  $300 \text{ A/cm}^2$ . This value is a rough, upper estimate of the true current density which at present was not possible to measure with the accuracy obtained in the JEOL 200B microscope. As the aim of this preliminary experiment was to check the hypothesis of defects diffusion from the amorphous side, the estimate served just to be sure that no appreciable sample heating might occur during irradiation. In fact, from Eq. (1), with  $k = 0.01 \text{ W cm}^{-1} \text{ K}^{-1}$ , which is the value of thermal conductivity of amorphous Si,  $r_0 = 5 \times 10^{-7} \text{ cm}$  and  $J = 300 \text{ A/cm}^2$ , it can be deduced that this condition is fulfilled. Moreover this estimate was confirmed by the absence of any appreciable recrystallization during irradiation in the same conditions with an energy of 100 keV.

The result obtained after irradiation with 200 keV electron for a time of 15 min is shown in Fig. 6. It is clear that epitaxial recrystallization took place, starting from the two  $a$ - $c$  interfaces and propagating to the beam impact region.<sup>24</sup> This gives ultimate evidence that (i) defects produced in the amorphous region contribute to particle-induced recrystallization; (ii) defects responsible for enhanced growth reach the  $a$ - $c$  interface by a diffusive process characterized by a diffusion length of some tens of nm.

#### IV. CONCLUSIONS

The main results obtained in this work by using cross-sectional electron microscopy technique may be summarized as follows.

The dominant mechanism of room-temperature electron-beam induced solid-phase epitaxy of amorphous silicon layers is the diffusion to the  $a$ - $c$  interface of the defects produced by irradiation both in the crystalline and in the amorphous regions.

The diffusion length of such defects is about 25–30 nm at room temperature, and seems to be approximately the same in both the amorphous and in the crystal. This fact, together with the observation that the contribution to regrowth coming from the crystal and from the amorphous are about the same, indicates a damage production rate which appears to be independent of the Si phase. Then, as concerns the production and diffusion of point defects under irradiation, amorphous and crystalline Si display a similar behavior.

Electron-beam irradiation induces polycrystalline nucleation at room temperature in the amorphous layer. This process is competitive with the induced solid-phase epitaxy when the dose is higher than  $5 \times 10^5$  C/cm<sup>2</sup>.

The role of cross-sectional electron microscopy as a powerful technique for the investigation of electron-

induced reactions in silicon has been demonstrated. Among the advantages that it offers in comparison with other experimental approaches, we can mention the *in situ* observation of the processes; the possibility of using electron energies both lower and higher than the threshold energy for atomic displacement, which makes it easy to clarify the role of point defects in the processes; the large beam current density ( $> 100$  A/cm<sup>2</sup>) available in a small spot, which allows a very high defect production rate without beam heating of the sample; the possibility to select with a resolution up to some nanometers the region where to produce point defects.

#### ACKNOWLEDGMENTS

Thanks are due to Mr. A. Bartolucci Ponti and to P. Battaini of Centro Ricerche Tecniche e Nucleari (CRTN) [Ente Nazionale per l'Energia Elettrica (ENEL), Milano, Italy], for their technical assistance. This work was supported by CNR, Progetto Finalizzato Materiali e Dispositivi per l'Elettronica a Stato Solido.

- <sup>1</sup>N. N. Gerasimenko, A. V. Dvurechenskii, G. A. Kachurin, N. B. Pridachin, and L. S. Smirnov, *Fiz. Tekh. Poluprovodn.* **6**, 1834 (1972) [*Sov. Phys.—Semicond.* **6**, 1588 (1973)].
- <sup>2</sup>J. Linnros, B. Svensson, and G. Holmén, *Phys. Rev. B* **30**, 3629 (1984).
- <sup>3</sup>R. G. Elliman, S. T. Johnson, A. P. Pogany, and J. S. Williams, *Nucl. Instrum. Methods B* **7/8**, 310 (1985).
- <sup>4</sup>G. Cembali, P. G. Merli, and F. Zignani, *Appl. Phys. Lett.* **38**, 808 (1981).
- <sup>5</sup>M. Berti, A. V. Drigo, G. Lulli, P. G. Merli, and M. Vittori Antisari, *Phys. Status Solidi A* **94**, 85 (1986).
- <sup>6</sup>M. Berti, A. V. Drigo, G. Lulli, P. G. Merli, and M. Vittori Antisari, *Phys. Status Solidi A* **97**, 77 (1986).
- <sup>7</sup>J. Linnros and G. Holmén, *J. Appl. Phys.* **59**, 1513 (1986).
- <sup>8</sup>J. S. Williams, R. G. Elliman, W. L. Brown, and T. E. Seidel, *Phys. Rev. Lett.* **55**, 1482 (1985).
- <sup>9</sup>V. E. Cosslett, in *Electron Microscopy and Analysis 1979*, edited by T. Mulvey (IOP, London, 1979), p. 277.
- <sup>10</sup>M. D. Matthews and S. J. Ashby, *Philos. Mag.* **27**, 1313 (1973).
- <sup>11</sup>J. Suski, L. Csepregi, J. Gyulai, H. Rzewuski, and Z. Werner, *Radiat. Eff.* **29**, 137 (1976).
- <sup>12</sup>J. Washburn, C. S. Murty, D. Sadana, P. Byrne, R. Gronsky, N. Cheung, and R. Kilaas, *Nucl. Instrum. Methods* **209/210**, 345 (1983).
- <sup>13</sup>M. Miyao, A. Polman, W. Sinke, F. W. Saris, and R. Van Kemp, *Appl. Phys. Lett.* **48**, 1132 (1986).
- <sup>14</sup>G. Lulli, P. G. Merli, M. Vittori Antisari, and B. Jouffrey, in *Proceedings of the 11th International Congress on Electron Microscopy*, edited by T. Imura, S. Maruse, and T. Suzuki (The Japanese Society of Electron Microscopy, Tokyo, 1986), Vol. II, p. 985.
- <sup>15</sup>W. A. McKinley and H. Feshbach, *Phys. Rev.* **74**, 1759 (1948).
- <sup>16</sup>L. W. Hobbs, in *Quantitative Electron Microscopy*, edited by J. H. Chapman and A. J. Craven (The University of Edinburgh, Edinburgh, 1983), p. 399.
- <sup>17</sup>Multiple displacements, which can occur for electron energies higher than the threshold energy for divacancy formation (i.e.,  $\sim 350$  keV), create defects which are in close proximity with one another and have high probability to interact and to form aggregates (Ref. 18). The activation energy for the motion of such aggregates is higher than the migration energy of isolated defects (Ref. 19). For instance, the simple divacancy is stable up to 300°C in Si. The consequence is that defects aggregates are not likely to give a contribution to the recrystallization process at room temperature. Moreover Corbett and Watkins (Ref. 18) have shown that the number of defect aggregates produced in Si by electron irradiation up to 2 MeV at room temperature is a small fraction of the total defects.
- <sup>18</sup>J. W. Corbett and G. D. Watkins, *Phys. Rev.* **2**, A555 (1965).
- <sup>19</sup>M. L. Swanson, in *Radiation Effects in Semiconductors*, edited by F. L. Vook (Plenum, New York, 1968), p. 46.
- <sup>20</sup>J. S. Williams and R. G. Elliman, *Appl. Phys. Lett.* **37**, 9 (1980).
- <sup>21</sup>J. A. Roth, S. A. Kokorowski, G. L. Olson, and L. D. Hess, in *Laser and Electron Beam Interactions with Solids*, edited by R. B. Appleton and G. K. Celler (North-Holland, New York, 1982), p. 169.
- <sup>22</sup>J. C. Bourgoin and P. Germain, *Phys. Lett.* **54A**, 444 (1975).
- <sup>23</sup>G. Lulli, P. G. Merli, and M. Vittori Antisari (unpublished).
- <sup>24</sup>A beam broadening, due to scattering effects, greater than the width of the amorphous layer should be excluded. In fact microdiffractions obtained with a beam spot of 10 nm centered in the middle of the amorphous region do not display any evidence of crystalline pattern.

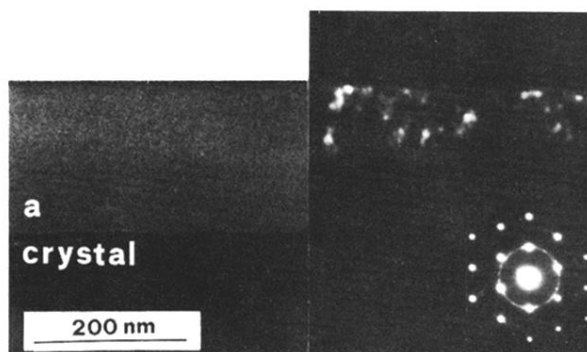


FIG. 3. TEM micrographs of a cross section of the sample irradiated at 200 keV under conditions described in Fig. 2. Left side, unirradiated area (bright-field image); a, amorphous region; right side, picture of the area irradiated with a dose of  $5 \times 10^5$  C/cm<sup>2</sup>. The latter picture is a dark-field image obtained using a portion of a polycrystalline ring present in the diffraction pattern reported in the inset.

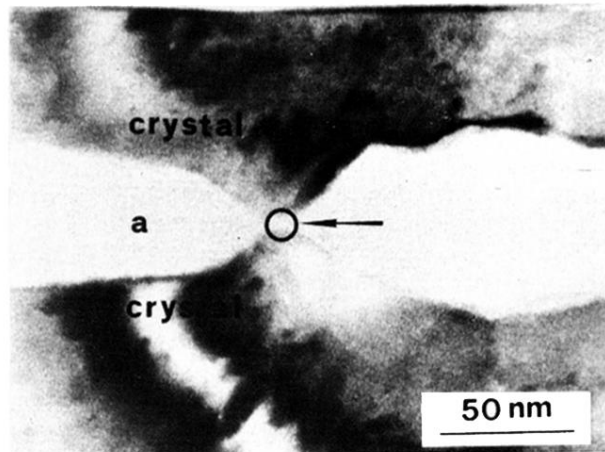


FIG. 6. TEM bright-field image of the sample irradiated at the center of the buried amorphous layer for a time of 15 min with a beam diameter of 10 nm. The arrow shows the beam impact region while the small ring represents the beam size; a, amorphous region. Beam energy was 200 keV. The current density was estimated of the order of 300 A/cm<sup>2</sup>.